Inorg. Chem. **2006**, *45*, 6479–6489

meso-Porphyrinylphosphine Oxides: Mono- and Bidentate Ligands for Supramolecular Chemistry and the Crystal Structures of Monomeric {[10,20-Diphenylporphyrinatonickel(II)-5,15-diyl]-bis-[P(O)Ph$_2$] and Polymeric Self-Coordinated {[10,20-Diphenylporphyrinatozinc(II)-5,15-diyl]-bis-[P(O)Ph$_2$]}

Farzad Atefi,[†] John C. McMurtrie,[†] Peter Turner,[‡] Martin Duriska,[§] and Dennis P. Arnold*,[†]

Synthesis and Molecular Recognition Program, School of Physical and Chemical Sciences, Queensland University of Technology, GPO Box 2434, Brisbane 4001, Australia, Crystal Structure Analysis Facility, School of Chemistry, University of Sydney, NSW 2006, Australia and School of Chemistry, Monash University, Victoria 3800, Australia

Received March 6, 2006

A series of porphyrins substituted in one or two meso positions by diphenylphosphine oxide groups has been prepared by the palladium-catalyzed reaction of diphenylphosphine or its oxide with the corresponding bromoporphyrins. Compounds {MDPP–[P(O)Ph$_2$]$_n$} (M = H$_2$, Ni, Zn; H$_2$DPP = 5,15-diphenylporphyrin; n = 1, 2) were isolated in yields of 60–95%. The reaction is believed to proceed via the conventional oxidative addition, phosphination, and reductive elimination steps, as the stoichiometric reaction of η^1-palladio(II) porphyrin [PdBr(H$_2$-DPP)(dppe)] (H$_2$DPP = 5,15-diphenylporphyrin; dppe = 1,2-bis(diphenylphosphino)ethane) with diphenylphosphine oxide also results in the desired mono-porphyrinylphosphine oxide [H$_2$DPP–P(O)Ph$_2$]. Attempts to isolate the tertiary phosphines failed due to their extreme air-sensitivity. Variable-temperature ^{1}H NMR studies of [H$_2$DPP–P(O)Ph$_2$] revealed an intrinsic lack of symmetry, while fluorescence spectroscopy showed that the phosphine oxide group does not behave as a "heavy atom" quencher. The electron-withdrawing effect of the phosphine oxide group was confirmed by voltammetry. The ligands were characterized by multinuclear NMR and UV–visible spectroscopy, as well as mass spectrometry. Single-crystal X-ray crystallography showed that the bis(phosphine oxide) nickel(II) complex {[NiDPP–[P(O)Ph$_2$]$_2$} is monomeric in the solid state, with a ruffled porphyrin core and the two P═O fragments on the same side of the average plane of the molecule. On the other hand, the corresponding zinc(II) complex formed infinite chains through coordination of one Ph$_2$PO substituent to the neighboring zinc porphyrin through an almost linear P═O···Zn unit, leaving the other Ph$_2$PO group facing into a parallel channel filled with disordered water molecules. These new phosphine oxides are attractive ligands for supramolecular porphyrin chemistry.

Introduction

Due to their central role in the photosynthetic process of plants and bacteria, porphyrins have attracted the attention of scientists from various backgrounds.[1] Although many synthetic challenges have been overcome in the past decade, the introduction of heteroatoms directly attached to the carbon framework of porphyrinoid macrocycles has almost exclusively been limited to nitrogen, oxygen, sulfur, and the halides.[2] Boron porphyrins have also been isolated in the past decade[3] and are now used as synthons in transition-

* To whom correspondence should be addressed. Email: d.arnold@qut.edu.au.
[†] Queensland University of Technology.
[‡] University of Sydney.
[§] Monash University.

(1) (a) *The Porphyrin Handbook*; Kadish, K. M., Smith, K. M., Guilard, R., Eds.; Academic Press: New York, 2000; Vol. 1−10. (b) *The Porphyrin Handbook*; Kadish, K. M., Smith, K. M., Guilard, R., Eds.; Academic Press: New York, 2004; Vol. 11−20.
(2) Vicente, M. G. H. In *The Porphyrin Handbook*; Kadish, K. M., Smith, K. M., Guilard, R., Eds.; Academic Press: San Diego, 2000; Vol. 1, pp 149−199.
(3) Hyslop, A. G.; Kellett, M. A.; Iovine, P. M.; Therien, M. J. *J. Am. Chem. Soc.* **1998**, *120*, 12676−12677.

10.1021/ic060372u CCC: $33.50
Published on Web 07/14/2006

metal-catalyzed reactions. Just recently, a method for highly regioselective β-borylation of disubstituted porphyrins has been introduced.[4] The formation of porphyrin mercurials was reported more than 20 years ago,[5] and these compounds were recently rediscovered by our group as transmetallating agents.[6] One isolated example of a porphyrinyl arsonium salt can also be found in the literature,[7] as well as a meso substituted tellurioporphyrin which was observed as an intermediate in the formation of a doubly directly linked porphyrin dimer.[8] The only examples of compounds with transition metal fragments directly attached to porphyrins have been isolated by our group.[9]

Phosphine oxides are well-established ligands for a variety of purposes[10] and are, for example, an integral part in the removal of radioactive waste from solutions.[11] Although there has been one report where a phosphine oxide has been directly attached to a phthalocyanine,[12] no such examples exist for porphyrins. The formation of a phosphine oxide attached to the meso position of an octaethylporphyrin via a methylene spacer was observed by us during an attempt to obtain an ylide from a porphyrinylmethylphosphonium iodide,[13] while a Japanese group[14] reported a phosphine oxide attached to a porphyrin via a biphenyl spacer group. Few examples of phosphines attached to the meso position of porphyrinyl macrocycles but separated by phenyl spacers have been reported in the literature, with a *meso*-tetrakis[4-(diphenylphosphino)phenyl]porphyrin being the first.[15] The authors described the extremely fast autoxidation of this compound and therefore reported the crystal structure of its tetraoxide. However, under strict exclusion of oxygen, a cubelike octakis(phosphonium salt) was obtained directly from the porphyrinylphosphine. In a second example of this class, the phosphine is separated from the porphyrin macrocycle by an alkynyl−phenyl spacer.[16a] Again, the authors report the phosphine to be very air-sensitive. Consequently, the product was protected in situ as the borane complex. The formation of porphyrin dimers, trimers, and tetramers with Ru(II)[16b−d] and Rh(III) porphyrins,[16e,f] as well as the formation of primary porphyrinylphosphines,[16g] have been reported by the same group. The most recent example of a porphyrinylphosphine described in the literature is a bis-phosphine in which biphenyl spacers separate the phosphine groups from the carbon backbone of the macrocycle.[17] In this case, the authors do not mention any complications due to oxidation processes. However, the product was isolated via a phosphine sulfide intermediate and the crystal structure of this sulfide was reported, rather than that of the phosphine itself. Thus, the air sensitivity of this compound seems to be self-evident. The formation of a tris(zinc(II) porphyrin)-phosphite ligand has also been reported recently.[18] Interestingly, the authors report that the phosphorus donor atom of this ligand does not coordinate to zinc(II) porphyrins and is therefore accessible for selective coordination, in this case to a Rh(I) catalyst.

Until now, the only examples of phosphorus atoms directly attached to the carbon framework of porphyrinoids remain phosphonium salts. A phthalocyanine−phosphonium salt has been obtained with a modest yield of 15% via a palladium-catalyzed reaction. Under the same reaction conditions, a bisphthalocyanine−phosphonium salt was obtainable in 50% yield and the authors could even successfully isolate a trisphthalocyanine−phosphonium salt with a modest yield of 9%.[19] Smith and co-workers reported the only example of a porphyrin−phosphonium salt in which the phosphorus atom is directly bonded to the meso position of the macrocycle,[7] while Shine's group reported under similar conditions the formation of a β-bonded phosphonium salt.[20] In both cases, the porphyrin cation radical intermediate was obtained chemically. A French group generated their porphyrin cation radicals electrochemically to obtain a phosphonium salt, in which the phosphorus is also β-bonded to the macrocycle.[21a] The same group reported under similar

(4) Hata, H.; Shinokubo, H.; Osuka, A. *J. Am. Chem. Soc.* **2005**, *127*, 8264−8265.

(5) Smith, K. M.; Langry, K. C. *J. Chem. Soc., Chem. Commun.* **1980**, 217−218.

(6) Kato, A.; Arnold, D. P.; Miyasaka, H.; Yamashita, M.; Sugiura, K.-i. unpublished results.

(7) Smith, K. M.; Barnett, G. H.; Evans, B.; Martynenko, Z. *J. Am. Chem. Soc.* **1979**, *101*, 5953−5961.

(8) Sugiura, K.-i.; Matsumoto, T.; Ohkouchi, S.; Naitoh, Y.; Kawai, T.; Takai, Y.; Ushiroda, K.; Sakata, Y. *J. Chem. Soc., Chem. Commun.* **1999**, 1957−1958.

(9) (a) Arnold, D. P.; Sakata, Y.; Sugiura, K.-i.; Worthington, E. I. *J. Chem. Soc., Chem. Commun.* **1998**, 2331−2332. (b) Arnold, D. P.; Healy, P. C.; Hodgson, M. J.; Williams, M. L. *J. Organomet. Chem.* **2000**, *607*; 41−50. (c) Hodgson, M. J.; Healy, P. C.; Williams, M. L.; Arnold, D. P. *J. Chem. Soc., Dalton Trans.* **2002**, 4497−4504. (d) Hartnell, R. D.; Arnold, D. P. *Organometallics* **2004**, *23*, 391−399. (e) Hartnell, R. D.; Arnold, D. P. *Eur. J. Inorg. Chem.* **2004**, 1262−1269. (f) Hartnell, R. D.; Edwards, A. J.; Arnold, D. P. *J. Porphyrins Phthalocyanines* **2002**, *6*, 695−707.

(10) See for example: (a) Karayannis, N. M.; Mikulski, C. M.; Pytlewski, L. L. *Inorg. Chim. Acta, Rev.* **1971**, *5*, 69−105. (b) Sterenberg, B. T.; Scoles, L.; Carty, A. J. *Coord. Chem. Rev.* **2002**, *231*, 183−197.

(11) Arnaud-Neu, F.; Browne, J. K.; Byrne, D.; Marrs, D. J.; McKervey, M. A.; O'Hagan, P.; Schwing-Weill, M. J.; Walker, A. *Chem.−Eur. J.* **1999**, *5*, 175−186.

(12) Märkl, G.; Gschwendner, K.; Roetzer, I.; Kreitmeier, P. *Helv. Chim. Acta* **2004**, *87*, 825−844.

(13) Yashunsky, D. V.; Ponomarev, G. V.; Arnold, D. P. *Tetrahedron Lett.* **1996**, *37*, 7147−7150.

(14) Sawamura, M.; Nakamura, E. In *74th Annual Meeting of the Chemical Society of Japan*; Chemical Society of Japan: Kyoto, 1998; p 4A315.

(15) Märkl, G.; Reiss, M.; Kreitmeier, P.; Noeth, H. *Angew. Chem., Int. Ed. Engl.* **1995**, *34*, 2230−2234.

(16) (a) Darling, S. L.; Stulz, E.; Feeder, N.; Bampos, N.; Sanders, J. K. M. *New J. Chem.* **2000**, *24*, 261−264. (b) Stulz, E.; Ng, Y.-F.; Scott, S. M.; Sanders, J. K. M. *J. Chem. Soc., Chem. Commun.* **2002**, 524−525. (c) Stulz, E.; Maue, M.; Feeder, N.; Teat Simon, J.; Ng, Y.-F.; Bond Andrew, D.; Darling Scott, L.; Sanders, J. K. M. *Inorg. Chem.* **2002**, *41*, 5255−5268. (d) Stulz, E.; Sanders, J. K. M.; Montalti, M.; Prodi, L.; Zaccheroni, N.; Fabrizi de Biani, F.; Grigiotti, E.; Zanello, P. *Inorg. Chem.* **2002**, *41*, 5269−5275. (e) Stulz, E.; Scott, S. M.; Ng, Y.-F.; Bond, A. D.; Teat, S. J.; Darling, S. L.; Feeder, N.; Sanders, J. K. M. *Inorg. Chem.* **2003**, *42*, 6564−6574. (f) Stulz, E.; Scott, S. M.; Bond, A. D.; Otto, S.; Sanders, J. K. M. *Inorg. Chem.* **2003**, *42*, 3086−3096. (g) Stulz, E.; Maue, M.; Scott, S. M.; Mann, B. E.; Sanders, J. K. M. *New J. Chem.* **2004**, *28*, 1066−1072.

(17) Saito, M.; Nishibayashi, Y.; Uemura, S. *Organometallics* **2004**, *23*, 4012−4017.

(18) Slagt, V. F.; van Leeuwen, P. W. N. M.; Reek, J. N. H. *Angew. Chem., Int. Ed.* **2003**, *42*, 5619−5623.

(19) De la Torre, G.; Gouloumis, A.; Vazquez, P.; Torres, T. *Angew. Chem., Int. Ed.* **2001**, *40*, 2895−2898.

(20) Shine, H. J.; Padilla, A. G.; Wu, S.-M. *J. Org. Chem.* **1979**, *44*, 4069−4075.

(21) (a) Ruhlmann, L.; Giraudeau, A. *J. Chem. Soc., Chem. Commun.* **1996**, 2007−2008. (b) Ruhlmann, L.; Giraudeau, A. *Eur. J. Inorg. Chem.* **2001**, 659−668. (c) Ruhlmann, L.; Gross, M.; Giraudeau, A. *Chem.−Eur. J.* **2003**, *9*, 5085−5096.

reaction conditions the formation of porphyrin dimers and trimers linked with diphosphonium and triphosphonium bridges, respectively.[21b,c]

From past reports, it seems evident that a directly linked porphyrinylphosphine would be prone to autoxidation and the isolation of such a compound would be at the best very problematic. Porphyrinylphosphine oxides on the other hand would not only be possible entry points for phosphines,[22] but they also could themselves be very interesting new building blocks for multi-porphyrin arrays, supramolecular systems that could give new insights into the photosynthetic reaction center.[23] Moreover, porphyrinylphosphine oxides are also interesting targets as ligands in other fields of coordination and organometallic chemistry. Bidentate phosphine oxides especially have undergone a renaissance in recent years due to the possibility of generating polymeric materials with interesting geometrical and physical properties.[24] We report here both stoichiometric and catalytic formation in excellent yields of a suite of porphyrin-based mono- and bis-phosphine oxides, as well as their physical and structural features, which clearly indicate the potential of these substances as building blocks for multi-porphyrin arrays.

Experimental Section

General Procedures and Instrumentation. All synthetic reactions involving zerovalent palladium metal reagents or phosphines were carried out in an atmosphere of high-purity argon using standard Schlenk techniques.[25] Chemical reagents and ligands were of laboratory reagent (LR) or analytical reagent (AR) grade, received from Sigma-Aldrich, and used without further purification. Solvents used were AR grade where available. Solvents used in palladium-catalyzed reactions were degassed by freeze/thawing three times prior to their use. Toluene and diethyl ether were stored over sodium wire. CH_2Cl_2 and $CHCl_3$ were stored over anhydrous sodium carbonate. Tetrahydrofuran (THF) was distilled immediately before use from a dark blue sodium/benzophenone solution under an atmosphere of high-purity argon. H_2DPP,[26] haloporphyrins **4**[27] and **7**,[28] *meso*-palladioporphyrin **5**,[9a] and palladium catalyst **18**[29] were synthesized according to the literature. Metals were inserted into the porphyrins following established procedures.[30] Recrystallization from two solvents was accomplished by dissolving the product in a minimum amount of the first solvent and carefully layering the solution with a 10-fold excess of the second solvent. Analytical TLC was performed using aluminum-backed Merck silica gel 60 F254 plates, and column chromatography was carried out using Merck silica gel (230−400 mesh). NMR spectra were recorded on a Bruker Avance 400 MHz instrument with $CHCl_3$ as internal standard at 7.26 ppm for ^{1}H spectra and 85% aqueous H_3PO_4 as external standard for proton-decoupled ^{31}P spectra. Quantitative UV/vis spectra were recorded on a Cary 3 spectrometer. Fluorescence spectra were recorded in dichloromethane solutions on a Varian Cary Eclipse fluorescence spectrophotometer equipped with a standard multicell Peltier thermostated sample holder. IR spectra were recorded on a Nicolet 870 Nexus Fourier transform infrared spectrometer equipped with a DTGS TEC detector and an ATR objective. High-accuracy electrospray ionization (ESI) mass spectra were recorded on a Bruker BioApex 47e FTMS fitted with an Analytica electrospray source. Dichloromethane was used as a solvent, and the samples were diluted either with dichloromethane/methanol or just methanol. The samples were introduced into the source by direct infusion (syringe pump) at 60 μL/h with a capillary voltage of 80 V. Sodium iodide clusters were used as internal standard for the calibration of the instrument. Laser desorption/ionization (LDI) MS analysis was performed with an Applied Biosystems Voyager-DE STR BioSpectrometry workstation. The instrument was operated in positive polarity in reflecton mode for analysis. Sample was spotted on a stainless steel sample plate and allowed to air-dry. Data from 500 laser shots (337 nm nitrogen laser) were collected, signal-averaged, and processed with the instrument manufacturer's Data Explorer software. Isotopic modeling was calculated by MassLynx V3.5 software by Micromass Limited. Elemental analyses were carried out by the Microanalytical Service, The University of Queensland.

Diphenyl(10,20-diphenylporphyrin-5-yl)phosphine Oxide (6) from 5. Porphyrin **5** (50 mg, 0.048 mmol), cesium carbonate (16 mg, 0.049 mmol), and **17** (10 mg, 0.049 mmol) were dried in a Schlenk flask under high vacuum. After the vessel was flushed three times with argon, toluene (7.5 mL) was added with a syringe and the reaction mixture was stirred at 84 °C under an atmosphere of argon for 4 h. The reaction mixture was loaded onto a column packed with silica gel in toluene. Palladium complexes and excess **17** were eluted with toluene before the solvent was changed to toluene/methanol (98:2). A dark red band was collected, and the solvents were removed in vacuo. Product **6** was obtained as dark purple crystals (27 mg, 0.041 mmol, 85%) after recrystallization from toluene/pentane. ^{1}H NMR (400 MHz, $CDCl_3$, 25 °C): δ 10.23 (s, 1H, *meso*-H), 9.55 (br d, 2H, β-H), 9.28, 8.86, 8.65 (d, ^3J(H,H) = 4.6 Hz, each 2H, β-H), 8.15−8.12 (m, 4H, *o*-H 10,20-phenyl), 7.90−7.85 (m, 4H, *o*-H PPh_2), 7.77−7.70 (m, 6H, *m*,*p*-H 10,20-phenyl), 7.53−7.49 (m, 2H, *p*-H PPh_2), 7.42−7.38 (m, 4H, *m*-H PPh_2), −2.54 (br s, 2H, NH). ^{31}P NMR (162 MHz, $CDCl_3$, 25 °C): δ 34.2. IR (ATR): $\tilde{\nu}$ [cm^{-1}] 1183 (P═O). UV/vis (CH_2Cl_2): λ_{max} [nm], (ϵ [10^3 mol^{-1} dm^3 cm^{-1}]) 416 (367), 514 (17.4), 548 (6.3), 586 (6.5), 639 (3.5). High-resolution ESI MS: *m*/*z* calcd for $[C_{44}H_{31}N_4OP + H]^+$: 663.2314; found: 663.2305. Anal. Calcd for $C_{44}H_{31}N_4OP$: C 79.74, H 4.71, N 8.45; found: C 79.89, H 4.81, N 8.19.

General Procedure for Palladium-Catalyzed Reactions. A Schlenk flask was charged with the porphyrin, cesium carbonate, and the catalyst **18**. Phosphine oxide **17** (105 mg, 0.51 mmol) was dissolved in toluene (50 mL) in a second Schlenk vessel to make up a stock solution. The appropriate amount of this solution was added to the porphyrin vessel with a syringe, and the reaction mixture was stirred at 84 °C. The mixture was loaded onto a column packed with silica gel in toluene. Palladium complexes and excess **17** were eluted before the solvent was changed to toluene/methanol. The major red band was collected, and the residue recrystallized as specified below.

(22) Engel, R. In *Handbook of Organophosphorus Chemistry*; Engel, R., Ed.; M. Dekker: New York, 1992; pp 193−239.
(23) Burrell, A. K.; Officer, D. L.; Plieger, P. G.; Reid, D. C. W. *Chem. Rev.* **2001**, *101*, 2751−2796.
(24) (a) Kim, S.-W.; Kim, S.; Tracy, J. B.; Jasanoff, A.; Bawendi, M. G. *J. Am. Chem. Soc.* **2005**, *127*, 4556−4557. (b) Spichal, Z.; Necas, M.; Pinkas, J. *Inorg. Chem.* **2005**, *44*, 2074−2080.
(25) Shriver, D. F.; Drezdzon, M. A. *The manipulation of air-sensitive compounds*; Wiley: New York, 1986.
(26) Laha, J. K.; Dhanalekshmi, S.; Taniguchi, M.; Ambroise, A.; Lindsey, J. S. *Org. Process Res. Dev.* **2003**, *7*, 799−812.
(27) Shanmugathasan, S.; Johnson, C. K.; Edwards, C.; Matthews, E. K.; Dolphin, D.; Boyle, R. W. *J. Porphyrins Phthalocyanines* **2000**, *4*, 228−232.
(28) DiMagno, S. G.; Lin, V. S. Y.; Therien, M. J. *J. Org. Chem.* **1993**, *58*, 5983−5993.
(29) Coulson, D. R. *Inorg. Synth.* **1971**, *13*, 121−124.
(30) Buchler, J. W. In *The Porphyrins*; Dolphin, D., Ed.; Academic Press: Vancouver, 1978; Vol. 1, pp 389−483.

Diphenyl(10,20-diphenylporphyrin-5-yl)phosphine Oxide (6). Porphyrin **4** (54 mg, 0.10 mmol), cesium carbonate (34 mg, 0.10 mmol), catalyst **18** (5 mg, 0.005 mmol), and **17** (23 mg, 0.11 mmol) in toluene (11 mL) gave, after 24 h of stirring, column chromatography (toluene/methanol = 98:2), and recrystallization from toluene/pentane, 64 mg of dark purple crystals (0.097 mmol, 97%).

(10,20-Diphenylporphyrin-5,15-diyl)bis(diphenylphosphine oxide) (12). Porphyrin **7** (31 mg, 0.050 mmol), cesium carbonate (34 mg, 0.10 mmol), catalyst **18** (5 mg, 0.005 mmol), and **17** (23 mg, 0.11 mmol) in toluene (11 mL) gave, after 40 h of stirring, column chromatography (toluene/methanol = 98:2), and recrystallization from toluene/pentane, 41 mg of dark purple crystals (0.048 mmol, 95%). ^{1}H NMR (400 MHz, $CDCl_3$, 25 °C): δ 9.43, 8.54 (d, ^3J(H,H) = 5.0 Hz, each 4H, β-H), 8.03−8.00 (m, 4H, *o*-H 10,20-phenyl), 7.91−7.86 (m, 8H, *o*-H PPh_2), 7.73−7.69 (m, 2H, *p*-H 10,20-phenyl), 7.67−7.62 (m, 4H, *m*-H 10,20-phenyl), 7.56−7.52 (m, 4H, *p*-H PPh_2), 7.45−7.40 (m, 8H, *m*-H PPh_2), −1.95 (br s, 2H, NH). ^{31}P NMR (162 MHz, $CDCl_3$, 25 °C): δ 32.9. IR (ATR): $\tilde{\nu}$ [cm^{-1}] 1184 (P═O). UV/vis (CH_2Cl_2): λ_{max} [nm], (ϵ [10^3 mol^{-1} dm^3 cm^{-1}]) 423 (289), 526 (10.5), 567 (14.0), 600 (6.3), 657 (10.5). High-resolution ESI MS: *m*/*z* calcd for $[C_{56}H_{40}N_4O_2P_2 + H]^+$: 863.2705; found: 863.2697. Anal. Calcd for $C_{56}H_{40}N_4O_2P_2$: C 77.95, H 4.67, N 6.49; found: C 77.89, H 4.84, N 6.28.

Diphenyl[10,20-diphenylporphyrinatonickel(II)-5-yl]phosphine Oxide (13). Porphyrin **8** (60 mg, 0.10 mmol), cesium carbonate (34 mg, 0.10 mmol), catalyst **18** (5 mg, 0.005 mmol), and **17** (23 mg, 0.11 mmol) in toluene (11 mL) gave, after 46 h of stirring, column chromatography (toluene/methanol = 98:2), and recrystallization from toluene/pentane, 69 mg of dark red crystals (0.096 mmol, 96%). ^{1}H NMR (400 MHz, $CDCl_3$, 25 °C): δ 9.73 (s, 1H, *meso*-H), 9.14, 9.07, 8.73, 8.51 (d, ^3J(H,H) = 4.9 Hz, each 2H, β-H), 7.91−7.89 (m, 4H, *o*-H 10,20-phenyl), 7.72−7.60 (m, 10H;, *m*,*p*-H 10,20-phenyl, *o*-H PPh_2), 7.36−7.31 (m, 4H, *m*-H PPh_2), 7.82−7.43 (m, 2H, *p*-H PPh_2). ^{31}P NMR (162 MHz, $CDCl_3$, 25 °C): δ 29.4. IR (ATR): $\tilde{\nu}$ [cm^{-1}] 1183 (P═O). UV/vis (CH_2Cl_2): λ_{max} [nm], (ϵ [10^3 mol^{-1} dm^3 cm^{-1}]) 414 (252), 538 (13.5), 578 (13.5). LDI MS: *m*/*z* calcd for $[C_{44}H_{29}N_4NiOP - H]^+$: 717.14; found: 717.17. Anal. Calcd for $C_{44}H_{29}N_4NiOP$: C 73.46, H 4.06, N 7.79; found: C 73.45, H 4.18, N 7.58.

[10,20-Diphenylporphyrinatonickel(II)-5,15-diyl]bis(diphenylphosphine oxide) (14). Porphyrin **9** (34 mg, 0.05 mmol), cesium carbonate (34 mg, 0.10 mmol), catalyst **18** (5 mg, 0.005 mmol), and **17** (23 mg, 0.11 mmol) in toluene (11 mL) gave, after 24 h of stirring, column chromatography (toluene/methanol = 98:2), and recrystallization from toluene/pentane, 44 mg of dark red crystals (0.048 mmol, 95%). ^{1}H NMR (400 MHz, $CDCl_3$, 25 °C): δ 9.07, 8.39 (d, ^3J(H,H) = 5.1 Hz, each 4H, β-H), 7.86−7.73 (m, 12H, *o*-H 10,20-phenyl, *o*-H PPh_2), 7.60−7.48 (m, 10 H, *m*,*p*-H 10,20-phenyl, *p*-H PPh_2), 7.41−7.37 (m, 8H, *m*-H PPh_2). ^{31}P NMR (162 MHz, $CDCl_3$, 25 °C): δ 29.2. IR (ATR): $\tilde{\nu}$ [cm^{-1}] 1181 (P═O). UV/vis (CH_2Cl_2): λ_{max} [nm], (ϵ [10^3 mol^{-1} dm^3 cm^{-1}]) 428 (167), 565 (7.2), 608 (16.2). LDI MS: *m*/*z* calcd for $[C_{56}H_{38}N_4NiO_2P_2 - H]^+$: 917.18; found: 917.21. Anal. Calcd for $C_{56}H_{38}N_4NiO_2P_2$: C, 73.14; H, 4.17; N, 6.09; found: C, 73.10; H, 4.22; N, 6.10.

Diphenyl[10,20-diphenylporphyrinatozinc(II)-5-yl]phosphine Oxide (15). Porphyrin **10** (60 mg, 0.10 mmol), cesium carbonate (34 mg, 0.10 mmol), catalyst **18** (5 mg, 0.005 mmol), and **17** (29 mg, 0.14 mmol) in toluene (14 mL) gave, after 24 h of stirring, column chromatography (toluene/methanol = 98:3), and recrystallization from toluene/MeOH/pentane, 44 mg of a dark purple powder (0.061 mmol, 61%). ^{1}H NMR (400 MHz, $CDCl_3$ + 1 drop pyridine-d_5, 25 °C): δ 10.17 (s, 1H, *meso*-H), 9.52, 9.27, 8.86, 8.63 (d, ^3J(H,H) = 4.6 Hz, each 2H, β-H), 8.11−8.09 (m, 4H, *o*-H 10,20-phenyl), 7.82−7.76 (m, 4H, *o*-H PPh_2), 7.70−7.64 (m, 6H, *m*,*p*-H 10,20-phenyl), 7.47−7.43 (m, 2H, *p*-H PPh_2), 7.35−7.30 (m, 4H, *m*-H PPh_2). ^{31}P NMR (162 MHz, $CDCl_3$ + 1 drop pyridine-d_5, 25 °C): δ 35.7. IR (ATR): $\tilde{\nu}$ [cm^{-1}] 1153 (P═O); after addition of pyridine to recrystallization: 1177 (P═O). UV/vis (CH_2Cl_2/5% pyridine): λ_{max} [nm], (ϵ [10^3 mol^{-1} dm^3 cm^{-1}]) 427 (267), 558 (9.4), 589 (4.8). LDI MS: *m*/*z* calcd for $[C_{44}H_{29}N_4OPZn - H]^+$: 723.13; found: 723.24.

Zinc(II) Phosphine Oxide 15 from 6. Porphyrin **6** (3.3 mg, 0.0049 mmol) was dissolved in CH_2Cl_2 (2 mL). Zinc acetate (3.3 mg, 0.021 mmol) dissolved in MeOH (1 mL) was added, and the reaction mixture was refluxed for 2 h. The precipitate was filtered and washed three times with MeOH to give 3.6 mg (ca. 100%) of a dark purple powder.

[10,20-Diphenylporphyrinatozinc(II)-5,15-diyl]bis(diphenylphosphine oxide) (16). Porphyrin **11** (17 mg, 0.025 mmol), cesium carbonate (17 mg, 0.055 mmol), catalyst **18** (2.5 mg, 0.0025 mmol), and **17** (12 mg, 0.055 mmol) in toluene (5.5 mL) gave, after 24 h of stirring, column chromatography (toluene/methanol = 98:5), and recrystallization from toluene/MeOH/pentane, 20 mg of dark purple crystals (0.022 mmol, 87%). ^{1}H NMR (400 MHz, $CDCl_3$ + 1 drop pyridine-d_5, 25 °C): δ 9.45, 8.50 (d, ^3J(H,H) = 4.9 Hz, each 4H, β-H), 7.99−7.96 (m, 4H, *o*-H 10,20-phenyl), 7.88−7.83 (m, 6H, *m*,*p*-H 10,20-phenyl), 7.80−7.75 (m, 8H, *o*-H PPh_2), 7.36−7.32 (m, 8H, *m*-H PPh_2), *p*-hydrogens of the PPh_2 group overlap with pyridine peaks. ^{31}P NMR (162 MHz, $CDCl_3$ + 1 drop pyridine-d_5, 25 °C): δ 34.8. IR (ATR, pyridine added to recrystallization): $\tilde{\nu}$[cm^{-1}] 1178 (P═O). UV/vis (CH_2Cl_2/5% pyridine): λ_{max} [nm], (ϵ [10^3 mol^{-1} dm^3 cm^{-1}]) 436 (315), 573 (8.4), 620 (17.0). LDI MS: *m*/*z* calcd for $[C_{56}H_{38}N_4O_2P_2Zn - H]^+$: 923.17; found: 923.23.

X-ray Single-Crystal Structure Determination of 14 and 16. Crystal data for **14** were collected at 150(2) K with ω and ϕ scans to approximately 56° 2θ using an APEXII-FR591 diffractometer employing graphite-monochromated Mo Kα radiation generated from a rotating anode (0.71073 Å). Data for **16** were collected at 103(2) K with ω and ϕ scans to approximately 45° 2θ using a Bruker Kappa diffractometer with SMART 6000 detector employing Double Diamond 111 monochromated radiation generated from a synchrotron. Data integration and reduction were undertaken with SAINT and XPREP,[31] and subsequent computations were carried out using the WinGX-32[32] graphical user interface. The structures were solved by direct methods using SIR97[33] then refined and extended with SHELXL-97.[34] Non-hydrogen atoms were refined anisotropically. Carbon-bound hydrogen atoms were included in idealized positions and were refined using a riding model. Hydrogen atoms attached to partial occupancy water molecules were not located in the difference Fourier map and have not been included in the refinement models. The refinement residuals are defined as $R1 = \sum||F_o| - |F_c||/\sum|F_o|$ for $F_o > 2\sigma(F_o)$ and $wR2 = \{\sum[w(F_o^2 - F_c^2)^2]/\sum[w(F_c^2)^2]\}^{1/2}$ where $w = 1/[\sigma^2(F_o^2) + (AP)^2 + BP]$, $P = (F_o^2 + 2F_c^2)/3$ and *A* and *B* are listed with the crystal data for each structure (Table 1).

Results and Discussion

Synthesis and Characterization of *meso*-Porphyrinylphosphine Oxides. Traditionally, phosphine oxides are

(31) *SAINT and XPREP*; Bruker Nonius Analytical X-ray Instruments, Inc.: Madison, WI, 2003.
(32) Farrugia, L. J. *J. Appl. Crystallogr.* **1999**, *32*, 837−838.
(33) Altomare, A.; Burla, M. C.; Camalli, M.; Cascarano, G. L.; Giacovazzo, C.; Guagliardi, A.; Moliterni, A. G. G.; Polidori, G.; Spagna, R. *J. Appl. Crystallogr.* **1999**, *32*, 115−119.
(34) Sheldrick, G. M. *SHELXL-97*; University of Göttingen: Göttingen, Germany, 1998.

Table 1. Experimental Crystallographic Data for **14** and **16**

	14	**16**
formula	$C_{56}H_{40}N_4NiO_3P_2$	$C_{56}H_{41}N_4O_{35}P_2Zn$
M_w	937.57	953.24
cryst color	dark red	dark purple
cryst size (mm^3)	$0.291 \times 0.085 \times 0.052$	$0.110 \times 0.020 \times 0.008$
cryst syst	monoclinic	monoclinic
recryst from	toluene/pentane	toluene/MeOH/pentane
space group	*C*2/*c* (No. 15)	$P2_1/c$ (No. 14)
a (Å)	20.2401(7)	19.984(3)
b (Å)	18.7057(7)	9.8207(14)
c (Å)	16.0264(6)	27.682(5)
β (deg)	123.651(2)	95.812(7)
V ($Å^3$)	5050.9(3)	4593.5(13)
Z	4	4
D_{calcd} (g cm^{-3})	1.233	1.378
λ (Å)	0.71073	0.48595
μ (mm^{-1})	0.495	0.494
$2\theta_{max}$	56.58	45.12
hkl range	−26 to 26, −24 to 24, −21 to 21	−26 to 25, −15 to 14, −43 to 43
N	39 751	130 658
N_{ind}	6262 ($R_{merge} = 0.142$)	17 545 ($R_{merge} = 0.114$)
N_{obs} ($I > 2\sigma(I)$)	3410	9860
N_{var}	309	608
R1(*F*, 2σ)	0.055	0.0497
wR2(F^2, all)	0.1547	0.1279
A	0.084	0.083
B	0.0	0.0
GOF (all)	0.934	0.907
$\Delta\rho_{min/max}$(e $Å^{-3}$)	−0.276/0.536	−0.294/1.176

prepared from lithium or Grignard reagents.[35] Unfortunately, no lithiated porphyrin macrocycle has been reported in the literature. The only example of a *meso*-magnesioporphyrin is mentioned in a patent.[36] In 1980, Hirao and co-workers reported the first palladium-catalyzed formation of a P−C bond.[37] In the past 25 years, this methodology has emerged to be one of the most versatile, mild, and effective approaches to generate various phosphonates, phosphites, phosphine oxides, and phosphines.[38] Although widely used in porphyrin chemistry to generate new C−C bonds,[39] there are fewer examples of the formation of heteroatom-substituted porphyrins promoted by Pd(0). Only boron,[3] nitrogen,[40] oxygen,[41] and sulfur[42] have been successfully coupled to porphyrinyl macrocycles. Nonetheless, we decided to pursue this avenue in order to synthesize the desired ligands.

Scheme 1. Formation of *meso*-Porphyrinylphosphine Oxide by the Stille Method

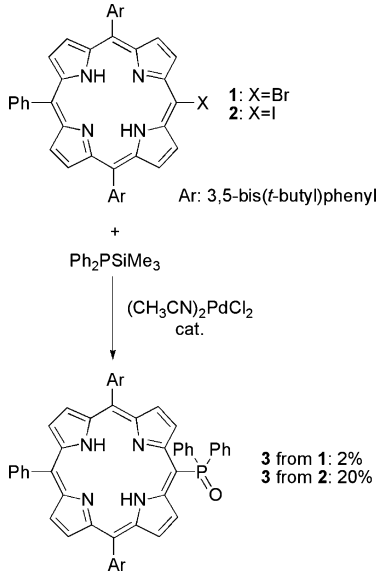

Our initial attempts to isolate *meso*-porphyrinyl phosphines by the method of Stille and co-workers[43] yielded the corresponding phosphine oxide in very low yields of 2%, if starting from bromoporphyrin **1**. Not surprisingly, the corresponding iodoporphyrin (**2**)[44] yielded the target compound in more respectable yield of 20%, as iodide is known to be more reactive in such processes.[45] (Scheme 1)

Although the major product of these reactions was always 5,15-bis(3,5-di-*tert*-butylphenyl)-10-phenylporphyrin (H_2-

(35) Engel, R. *Handbook of organophosphorus chemistry*; M. Dekker: New York, 1992.
(36) Therien, M. J. International Patent, WO 02/104072, 2002.
(37) Hirao, T.; Masunaga, T.; Ohshiro, Y.; Agawa, T. *Tetrahedron Lett.* **1980**, *21*, 3595−3598.
(38) For recent reviews see: (a) Hartwig, J. F. In *Handbook of Organopalladium Chemistry for Organic Synthesis*; Negishi, E.-i., Ed.; John Wiley and Sons: 2002; Vol. 1, pp 1051−1096. (b) Schwan, A. L. *Chem. Soc. Rev.* **2004**, *33*, 218−224.
(39) See for example: (a) Sharman, W. M.; Van Lier, J. E. *J. Porphyrins Phthalocyanines* **2000**, *4*, 441−453. (b) Setsune, J.-i. *J. Porphyrins Phthalocyanines* **2004**, *8*, 93−102.
(40) (a) Gao, G. Y.; Chen, Y.; Zhang, X. P. *J. Org. Chem.* **2003**, *68*, 6215−6221. (b) Takanami, T.; Hayashi, M.; Hino, F.; Suda, K. *Tetrahedron Lett.* **2003**, *44*, 7353−7357. (c) Chen, Y.; Zhang, X. P. *J. Org. Chem.* **2003**, *68*, 4432−4438. (d) Gao, G.-Y.; Chen, Y.; Zhang, X. P. *Org. Lett.* **2004**, *6*, 1837−1840. (e) Esdaile, L. J.; McMurtrie, J. C.; Turner, P.; Arnold, D. P. *Tetrahedron Lett.* **2005**, *46*, 6931−6935.
(41) Gao, G.-Y.; Colvin, A. J.; Chen, Y.; Zhang, X. P. *Org. Lett.* **2003**, *5*, 3261−3264.
(42) Gao, G.-Y.; Colvin, A. J.; Chen, Y.; Zhang, X. P. *J. Org. Chem.* **2004**, *69*, 8886−8892.
(43) Tunney, S. E.; Stille, J. K. *J. Org. Chem.* **1987**, *52*, 748−753.
(44) Atefi, F.; Locos, O. B.; Senge, M. O.; Arnold, D. P. *J. Porphyrins Phthalocyanines* **2006**, *10*, 176−185.
(45) Tsuji, J. *Palladium reagents and catalysts: innovations in organic synthesis*; Wiley and Sons: Chichester; New York, 1996.

Scheme 2. Synthesis of *meso*-η^1-Palladioporphyrin

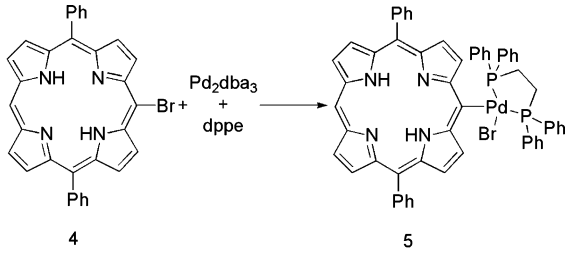

Scheme 3. Stoichiometric Formation of *meso*-Porphyrinylphosphine Oxide **6**

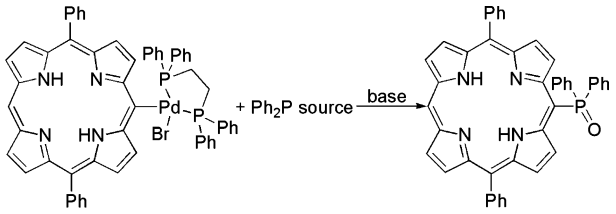

DAPP), these initial experiments supplied us with important insights into these reactions. As already expected, phosphines tend to oxidize very readily and rapidly in the presence of porphyrins to the corresponding phosphine oxide.[15,16a] The optimum reaction temperature for the formation of the new carbon−phosphorus bond is apparently ∼85 °C. At lower temperatures (<80 °C), no reactions were observed, while higher temperatures (>90 °C) favor the dehalogenation of the porphyrin, as do reaction times over 72 h. We also found that the phosphine oxide **3** is soluble in most common organic solvents except pentane.

To optimize our reaction conditions, it was decided to continue the experiments with a *meso*-η^1-palladioporphyrin as starting material. These *meso*-metalloporphyrins are readily available from a stoichiometric oxidative addition of a haloporphyrin with [Pd_2dba_3] (dba = dibenzylideneacetone) and a ligand, in this case dppe [dppe = 1,2-bis(diphenylphosphino)ethane][9b] (Scheme 2).

Palladioporphyrin **5** was chosen for several reasons. As the halogen is in the cis position to the porphyrin macrocycle, we anticipated it might increase the rate of our reactions and thus reduce the reaction times. We replaced the substituted aryl groups on the porphyrin by simple phenyls to lower the solubility of the target compound and therefore simplify the purification process. The remaining vacant meso position of the macrocycle provides the opportunity to carry out further reactions at a later stage. Palladioporphyrin **5** was reacted with various phosphines and phosphine oxides under different conditions, as shown in Scheme 3 and summarized in Table 2.

The first five entries underline our findings from the previous experiments that porphyrinylphosphines are readily and rapidly oxidized to the corresponding phosphine oxide. The widely used borane protecting group[46] seems in this case to be ineffective, although the Sanders group successfully protected their porphyrinylphosphine as such a complex.[16a]

(46) Imamoto, T.; Takeyama, T.; Kusumoto, T. *Chem. Lett.* **1985**, 1491−1492.

Table 2. Conditions and Yields (%) for Stoichiometric Reactions to Form **6**

Ph_2P source	base	yield[a]
Ph_2PH	−	<10
Ph_2PSiMe_3	−	<20
$Ph_2P(BH_3)H$	−	35
$Ph_2P(BH_3)H$	DBU[b]	<5
$Ph_2P(BH_3)H$	Cs_2CO_3	65
$Ph_2P(O)H$	−	70
$Ph_2P(O)H$	Cs_2CO_3	85

[a] Yield by ^{1}H NMR, purified yield only for last entry. [b] DBU = 1,5-diazabicyclo[5.4.0]undec-7-ene.

We assume that the oxidation of the phosphine is facilitated by the porphyrin itself, as already noted by Märkl and coworkers.[15] Both acidic and basic reagents can lead to the cleavage of the Pd−C bond in *meso*-palladioporphyrins.[47] DBU seems to promote this cleavage, and the major product in all cases, besides the desired porphyrinylphosphine oxide, was unsubstituted 5,15-diphenylporphyrin (H_2DPP). The last entry of Table 2 shows, however, that a heterogeneous base improves the yield of the desired product. Encouraged by this result, our next goal was to repeat these results under catalytic conditions (Scheme 4, Table 3).

It is important to note that these results are only reproducible using freshly prepared Pd(0) catalyst (**18**). Purification of the free base and nickel products was easily achieved, as the reaction mixture can be loaded onto a short silica column without removal of the solvent. Excess diphenylphosphine oxide **17** can be eluted with toluene, while the products are retained on the column. The addition of small amounts of MeOH is sufficient to elute the porphyrins. The lower yield for the zinc analogues (**15**, **16**) can be explained by the problematic purification process. Both of these ligands self-coordinate, as indicated to us by the lower solubility and slow elution of these products. Even higher amounts of MeOH still result in streaking on the column. These Zn(II) products are also very insoluble in organic solvents, and a mixture of toluene/MeOH with the aid of sonication is needed for recrystallization. Fortunately for the prospects of these porphyrins as ligands, these findings indicate a very strong O−metal coordination. Porphyrin **15** is also obtainable from its free base analogue **6** in almost quantitative yield by the standard metal insertion method with zinc acetate.

High-resolution ESI mass spectrometry (MS) was used as first evidence for the formation of the free base ligands (**6**, **12**), and indeed, the results confirmed the proposed formulations. As the metalated porphyrins (**13**−**16**) could not be protonated by ESI, we choose to perform LDI on them. This "harder" ionization technique leads in the case of phosphine oxides to the detection of an $(M - H)^+$ ion instead of the $(M + H)^+$ ion found for **6** and **12**. Williams et al.[48] studied the mass spectral fragmentation of various di- and triphenylphosphine oxides and concluded from isotopic labeling that the prominent $(M - H)^+$ fragments are cyclic quasi-

(47) Kato, A.; Hartnell, R. D.; Yamashita, M.; Miyasaka, H.; Sugiura, K.-i.; Arnold, D. P. *J. Porphyrins Phthalocyanines* **2005**, *8*, 1222−1227.
(48) Williams, D. H.; Ward, R. S.; Cooks, R. G. *J. Am. Chem. Soc.* **1968**, *90*,; 966−972.

Scheme 4. Catalytic Formation of *meso*-Porphyrinylphosphine Oxides

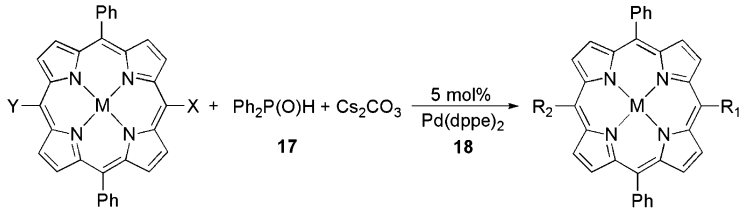

4: M=H_2; X=Br; Y=H
7: M=H_2; X=Br; Y=Br
8: M=Ni; X=Br; Y=H
9: M=Ni; X=Br; Y=Br
10: M=Zn; X=Br; Y=H
11: M=Zn; X=Br; Y=Br

6: M=H_2; R^1=P(O)Ph_2; R^2=H
12: M=H_2; R^1=P(O)Ph_2; R^2=P(O)Ph_2
13: M=Ni; R^1=P(O)Ph_2; R^2=H
14: M=Ni; R^1=P(O)Ph_2; R^2=P(O)Ph_2
15: M=Zn; R^1=P(O)Ph_2; R^2=H
16: M=Zn; R^1=P(O)Ph_2; R^2=P(O)Ph_2

Table 3. Conditions and Yields (%) for Catalytic Reactions

product	ratio halo-porphyrin/**17**	reaction time (h)	yield
6	1:1.1	24	>95
12	1:2.2	40	>95
13	1:1.1	46	>95
14	1:2.1	24	>95
15	1:1.4	24	61[a]
16	1:2.2	24	80[b]

[a] Yield by ^{1}H NMR higher, purification problematic. [b] ^{1}H NMR of reaction mixture shows only one porphyrin, purification problematic.

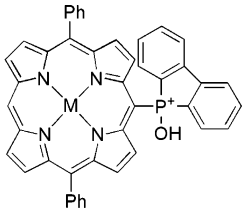

Figure 1. Quasi-onium ion.

onium ions, the analogues of which for our compounds would be the structure shown in Figure 1.

Traditionally, infrared spectroscopy (IR) has played a significant role in the characterization of phosphine oxides and their complexes due to the ease of observation of the strong P═O vibration [$\tilde{\nu}$(PO)]. IR is still a very useful tool for the identification of these ligands. Table 4 shows the collected $\tilde{\nu}$(PO) data for porphyrins **6** and **12**−**16** together with simpler models triphenylphosphine oxide ($OPPh_3$) and **17**.

Again, the two free base analogues **6** and **12** and the two nickel porphyrins **13** and **14** behave in a similar manner. The $\tilde{\nu}$(PO) for these compounds agree well with the literature values for Märkl's[12] phosphine oxide-substituted phthalocyanine. The decrease in $\tilde{\nu}$(PO) by ∼25 cm^{-1} for **15** can be explained by its self-coordination. Due to the interaction with a Lewis acidic metal ion, complexed phosphine oxides are known to have a lower $\tilde{\nu}$(PO) value.[49] After treatment of **15** and **16** with excess pyridine, the $\tilde{\nu}$(PO) value for the isolated solids indicates the presence of uncomplexed phosphine oxide ligand. Interestingly, Märkl and co-workers did not observe such a self-coordination feature for their zinc phthalocyanine.[12] The chemical shifts in the ^{31}P NMR spectra, between 29.2 and 35.7 ppm, also agree well with the values reported for the phthalocyanines.

Table 4. IR Frequencies (cm^{-1}) of Porphyrinylphosphine Oxides

compound	$OPPh_3$	**17**	**6**	**12**	**13**	**14**	**15**[a]	**15**	**16**[a]
$\tilde{\nu}$(PO)	1192	1192	1183	1184	1183	1182	1177	1153	1178

[a] Solid isolated after addition of pyridine to a solution in CH_2Cl_2.

Variable-Temperature ^{1}H NMR Studies of 6. The effects of the large delocalized aromatic system of porphyrins can be observed in their ^{1}H NMR spectra. Shielding of the inner nitrogen protons shifts the peaks representing them far upfield, while a deshielding effect shifts the peaks of the protons attached to the outer carbon skeleton downfield into the region of 8−11 ppm. Due to this feature, porphyrinyl compounds can be very easily detected by ^{1}H NMR spectroscopy, even in reaction mixtures. The spectrum of porphyrin **6** has an added interesting feature. Instead of the expected four doublets, each representing two β-protons, three doublets and a broad peak at ∼9.3 ppm can be observed. Two-dimensional ^{1}H NMR studies (dqf-COSY, NOESY) showed us that this broad peak represents the two protons next to the C−P bond. Intrigued by this phenomenon, we decided to conduct some variable-temperature ^{1}H NMR studies.

The spectra on the left-hand side of Figure 2 were recorded at 23−55 °C. The broad peak sharpens upon raising the temperature. By lowering the temperature (right-hand side of Figure 3, CD_2Cl_2 as solvent), all doublets broaden and at −40 °C no doublets can be observed. By lowering the temperature even further to −90 °C, instead of the four doublets, eight emerge. The arrows show the two peaks which diverge from the broad room-temperature peak. The peak representing the inner NH protons (−2.5 ppm) also splits into two signals at this low temperature. We attribute these features to the tautomerism of the inner N-protons. (Figure 3)

Similar features can be observed for meso-substituted porphyrins with other crowded substituents, like the *meso*-palladioporphyrins (e.g., **5**); however, the peak broadening in those compounds occurs at much lower temperatures (−30 °C).

Electronic Absorption Spectra, Emission Spectra, and Redox Properties. The main electronic absorption bands for the porphyrinylphosphine oxides (Figure 4, Table 5) show

(49) Cotton, F. A.; Barnes, R. D.; Bannister, E. *J. Chem. Soc.* **1960**, 2199−2203.

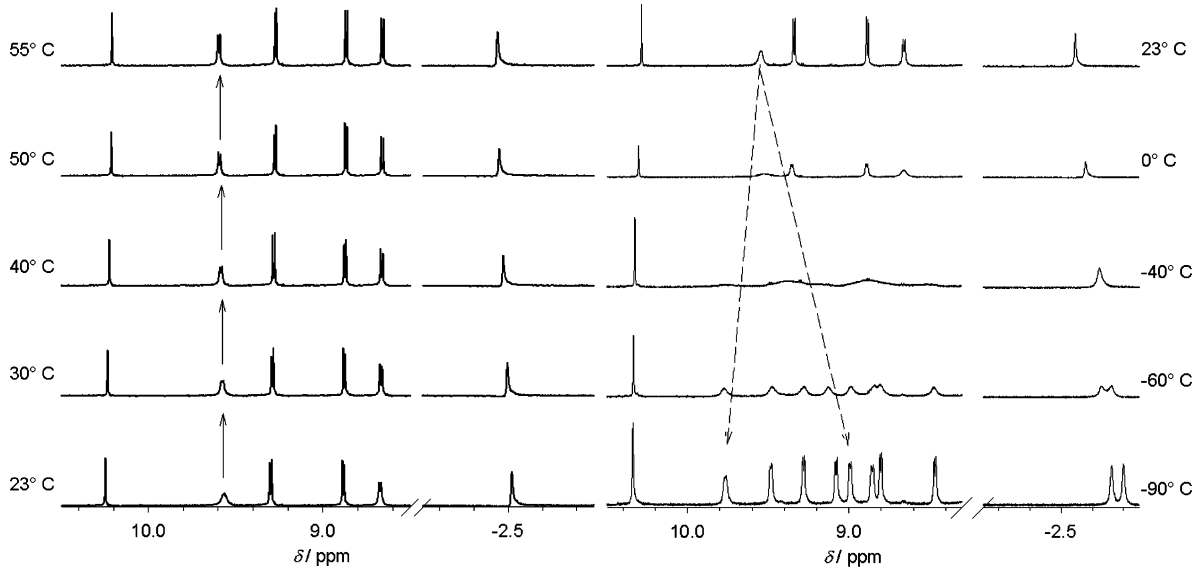

Figure 2. Variable-temperature ^{1}H NMR spectra in $CDCl_3$ (left) and CD_2Cl_2 (right) of **6**.

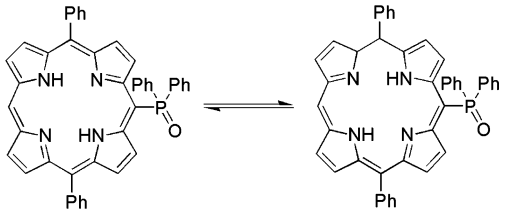

Figure 3. Tautomerism of inner N-protons.

the expected characteristics for substituted DPP.[50] Several trends can be recognized even in this limited set of data. A bathochromic shift in comparison to DPP[51] can be observed with increasing number of substituents. The shift is greatest for zinc porphyrins **15** and **16** followed by the nickelated compounds (**13**, **14**) and least for the free base porphyrins (**6**, **12**). As usual, the presence of a metal coordinated to the macrocycle raises its symmetry, which is reflected in only two observable *Q*-bands, instead of the four detected for the free base porphyrins.

We were also very much interested to explore whether the phosphine oxide substituent would have any effects on the fluorescence behavior of the macrocycle. Figure 5 shows the fluorescence spectra of the two free base porphyrins (**6**, **12**) together with the spectrum of H_2DPP for comparison. All three compounds were excited at their respective Soret band maxima, while the intensities are normalized to 0.1 absorbance. From these data, we calculated the fluorescence quantum efficiency (Φ) for the three porphyrins according to the comparative method.[52]

$$\Phi = \Phi_{\mathrm{std}} \times \frac{F}{F_{\mathrm{std}}} \times \frac{A_{\mathrm{std}}}{A}$$

where F is the fluorescence obtained by integrating the area underneath the curve and A represents the absorbance. As standard, the well-known quantum efficiency of 5,10,15,-20-tetraphenylporphyrin ($\Phi_{\mathrm{std}} = 0.11$) was used.[53] Our results indicate that increasing the number of substituents raises the quantum yield only slightly. The quantum yield of H_2DPP

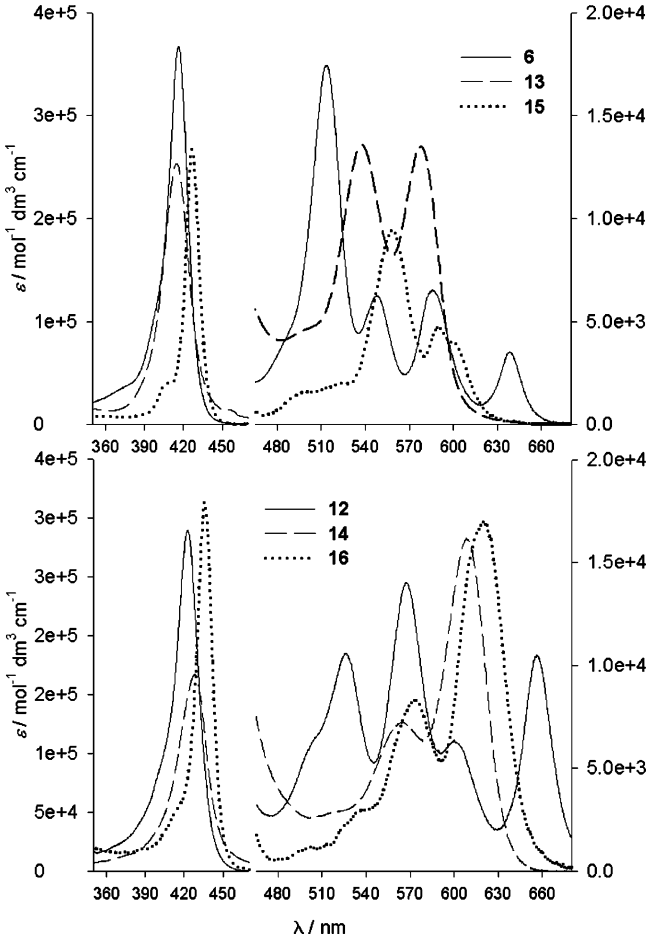

Figure 4. UV/vis absorption spectra for porphyrinyl phosphine oxides (in CH_2Cl_2 solution; with 5% pyridine for **15** and **16**).

(50) Ryppa, C.; Senge, M. O.; Hatscher, S. S.; Kleinpeter, E.; Wacker, P.; Schilde, U.; Wiehe, A. *Chem.*−*Eur. J.* **2005**, *11*, 3427−3442.
(51) Brückner, C.; Posakony, J. J.; Johnson, C. K.; Boyle, R. W.; James, B. R.; Dolphin, D. *J. Porphyrins Phthalocyanines* **1998**, *2*, 455−465.
(52) Ogunsipe, A.; Nyokong, T. *J. Porphyrins Phthalocyanines* **2005**, *9*, 121−129.
(53) Seybold, P. G.; Gouterman, M. *J. Mol. Spectrosc.* **1969**, *31*, 1−13.

Table 5. Wavelengths for the UV/vis Absorption Bands for Porphyrinylphosphine Oxides (in CH_2Cl_2 Solution; with 5% Pyridine for **15** and **16**)

	λ [nm]	
product	soret band	*Q*-bands
6	416	514, 548, 585, 639
12	423	526, 567, 600, 657
13	415	538, 578
14	428	565, 608
15	427	558, 589
16	436	573, 620

was calculated to be 0.07, while the addition of one substituent (**6**) raises this value to 0.08 and the second substituent (**12**) increases the quantum yield even further to 0.10. Notably, the diphenylphosphine oxide does not behave as a "heavy atom" quencher.

The redox properties of the free base oxides **6** and **12** were studied briefly by cyclic and square wave voltammetry at a Pt working electrode in CH_2Cl_2 containing 0.1 M Bu_4NPF_6. (vs Ag/Ag^+; ferrocene/ferrocinium couple at +0.55 V). While H_2DPP showed reversible first reduction and oxidation waves at −1.05 and +1.16 V, respectively,[9c] **6** was reduced at −0.96 V (reversible) and oxidized at +1.24 V (partly reversible). The corresponding data for bis-oxide **12**, were −0.73 and +1.33 V. These results indicate the electron-withdrawing properties of the phosphine oxide substituent-(s), which cause anodic shifts of both reduction and oxidation potentials.

Crystal Structures. Nickel(II) Bis(phosphine oxide) (14). In the crystal structure of **14** (Figure 6a), the complex has 2-fold crystallographic symmetry [Ni(II) on 2-fold special position with the 2-fold axis being normal to mean plane of the complex]. Selected geometric parameters are provided in Table 6. The nickel(II) center, which occupies the porphyrin cavity, is four coordinate and very close to square planar with a maximum deviation of N atoms from the mean N_4 plane of 0.034 Å. The porphyrin ring is significantly distorted from planarity (Figure 6b), having a distinctive saddle-like conformation. The maximum deviations from the mean plane of the macrocycle occur for the meso carbon atoms [distance; *meso*-C(5) to mean plane 0.814 Å, *meso*-C(10) to mean plane 0.747 Å], and as such, the porphyrin complex has the conformation type generally referred to as ruffled.[54] The diphenylphosphine oxide groups project on the same side of the macrocycle in a cis-like geometry.

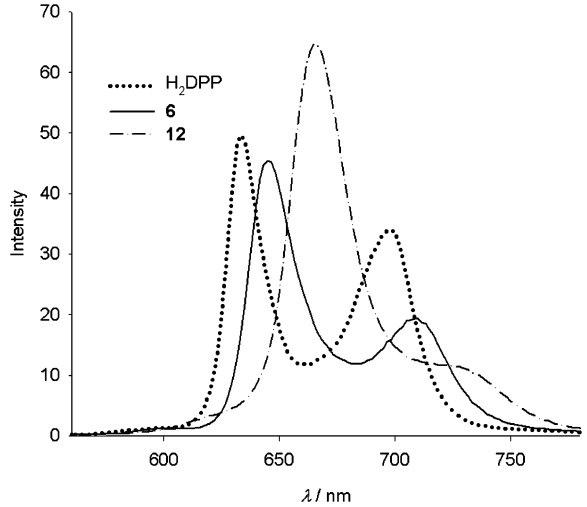

Figure 5. Fluorescence spectra of H_2DPP, **6**, and **12** (in CH_2Cl_2 solution).

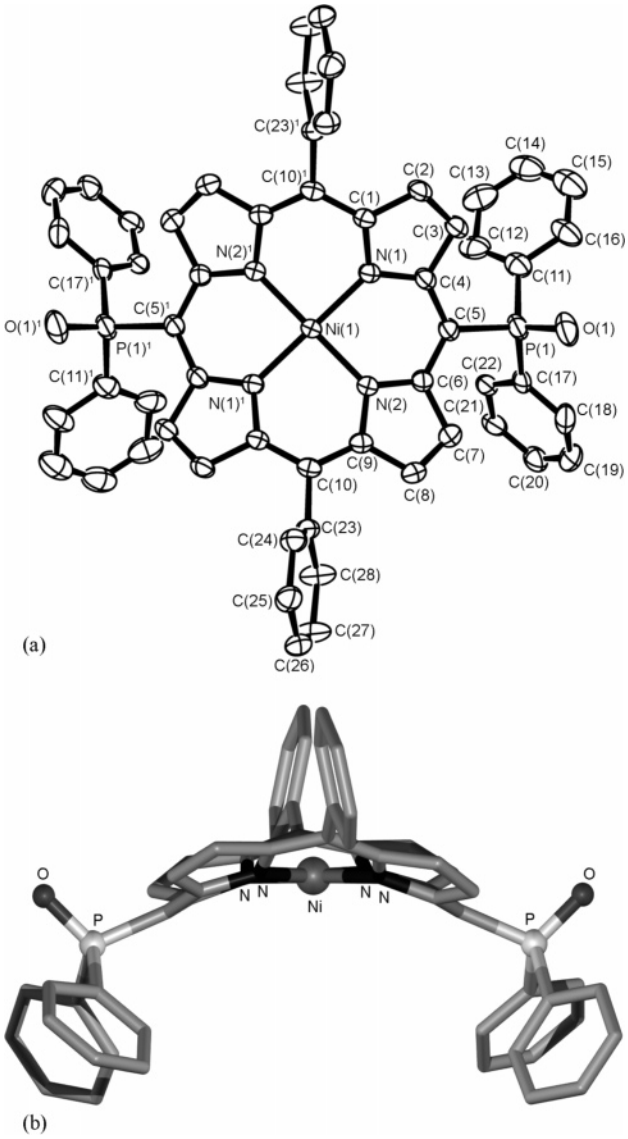

Figure 6. (a) ORTEP representation of {[10,20-diphenylporphyrinato-nickel(II)-5,15-diyl]-bis-[$P(O)Ph_2$}·H_2O. The complex has 2-fold symmetry ($1 - x, y, -z + 3/2$). Ellipsoids are depicted with 30% probability, and water and H atoms have been omitted. (b) Illustration of the {[10,20-diphenylporphyrinatonickel(II)-5,15-diyl]-bis-[$P(O)Ph_2$}·H_2O complex showing the almost perfect square planar coordination contrasting with the distorted macrocycle framework. Note also the cis-like arrangement of the diphenylphosphine oxide groups.

Table 6. Selected Bond Lengths (Å) and Angles (deg) for {[10,20-diphenylporphyrinatonickel(II)-5,15-diyl]-bis-[$P(O)Ph_2$}·H_2O

Ni(1)−N(1)	1.8941(19)	P(1)−C(5)	1.817(3)
Ni(1)−N(2)	1.891(2)	P(1)−C(11)	1.777(4)
P(1)−O(1)	1.487(2)	P(1)−C(17)	1.810(3)
N(2)[a]−Ni(1)−N(2)	179.19(13)	O(1)−P(1)−C(17)	110.93(14)
N(2)−Ni(1)−N(1)[a]	90.70(9)	C(11)−P(1)−C(17)	105.24(14)
N(2)−Ni(1)−N(1)	89.32(9)	O(1)−P(1)−C(5)	114.77(14)
N(1)[a]−Ni(1)−N(1)	176.81(12)	C(11)−P(1)−C(5)	105.42(14)
O(1)−P(1)−C(11)	111.15(15)	C(17)−P(1)−C(5)	108.77(11)

[a] $-x, y, -z + 3/2$.

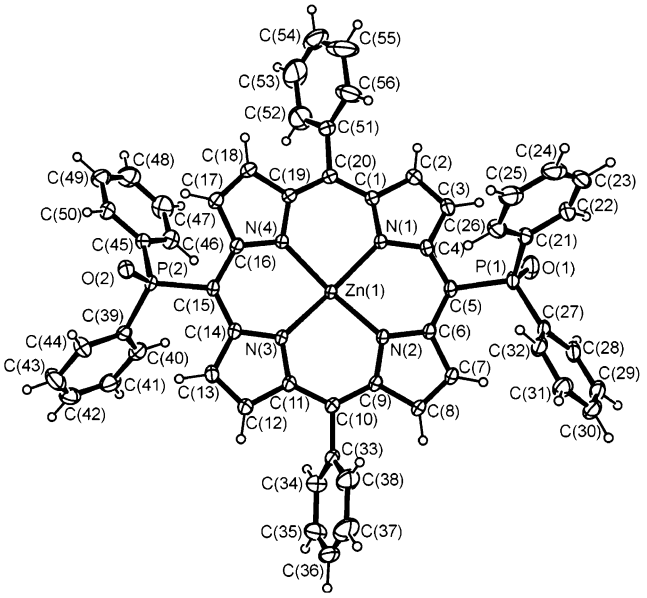

Figure 7. ORTEP representation of the asymmetric unit of {[10,20-diphenylporphyrinatozinc(II)-5,15-diyl]-bis-[P(O)Ph$_2$]}$_n$·{1.5H$_2$O}$_n$ 50% probability ellipsoids, disordered water omitted). The coordination sphere of the complex is shown in Figure 8.

The crystal structure of the nickel(II) complex **14** is characterized by a number of different aryl−aryl intermolecular interactions that involve diphenylphosphine oxide phenyl rings, the meso substituent phenyl rings, and the aromatic porphyrin framework. Notable interactions are described here. The meso substituent phenyl ring C(23)−C(28) is simultaneously involved in edge-to-face-type interactions with the aromatic porphyrin face of an adjacent complex (CH_{edge}···porphyrin face = 2.6 Å), the diphenylphosphine oxide phenyl group comprising C(11)−C(16) (CH_{edge}···Ph_{plane} = 2.7 Å) and the diphenylphosphine oxide phenyl group comprising C(17)−C(22) (CH_{edge}···Ph_{plane} = 3.3 Å). The complexes are organized in such a way as to create continuous channels that run parallel to the crystallographic *c* axis. These channels are filled with diffuse solvent molecules (modeled as partial occupancy water molecules, O(1w)−O(5w).

Zinc(II) Bis(phosphine oxide) (16). In the crystal structure of {[10,20-diphenylporphyrinatozinc(II)-5,15-diyl]-bis-[P(O)Ph$_2$]}$_n$·{1.5H$_2$O}$_n$, the asymmetric unit comprises a single zinc(II) porphyrin complex and 1.5 molecules of water that are positionally disordered over seven sites (O1w−O7w). An ORTEP[55] representation of the asymmetric unit is provided in Figure 7, and selected geometric data are provided in Table 7. The zinc(II) center [Zn(1)] is five-coordinate with approximate square pyramidal stereochemistry, as shown in Figure 8. The four nitrogen atoms of the macrocycle [N(1)−N(4)] are arranged in a square planar configuration with the maximum deviation from the mean N_4 plane occurring for N(4) [0.0355(8) Å]. The zinc(II) atom is located 0.321 Å from the mean N_4 plane, and the apical coordination site is occupied by an oxygen atom [O(2)] from one of the diphenylphosphine oxide groups of an adjacent

Table 7. Selected Bond Lengths (Å) and Angles (deg) for {[10,20-diphenylporphyrinatozinc(II)-5,15-diyl]-bis-[P(O)Ph$_2$]}$_n$·{1.5H$_2$O}$_n$

Zn(1)−N(1)	2.0805(15)	P(1)−C(21)	1.816(2)
Zn(1)−N(2)	2.0719(14)	P(1)−C(27)	1.7971(19)
Zn(1)−N(3)	2.0679(15)	P(2)−O(2)	1.4856(15)
Zn(1)−N(4)	2.0575(15)	P(2)−C(15)	1.8108(17)
Zn(1)−O(2)[a]	2.0224(14)	P(2)−C(39)	1.8054(19)
P(1)−O(1)	1.4899(17)	P(2)−C(45)	1.8048(19)
P(1)−C(5)	1.8353(18)		
N(1)−Zn(1)−N(2)	87.56(6)	O(1)−P(1)−C(21)	112.99(10)
N(1)−Zn(1)−N(3)	164.11(7)	O(1)−P(1)−C(27)	110.35(9)
N(1)−Zn(1)−N(4)	88.85(6)	C(5)−P(1)−C(21)	105.05(9)
N(1)−Zn(1)−O(2)[a]	97.97(6)	C(5)−P(1)−C(27)	111.58(9)
N(2)−Zn(1)−N(3)	90.46(6)	C(21)−P(1)−C(27)	102.41(9)
N(2)−Zn(1)−N(4)	160.09(6)	O(2)−P(2)−C(15)	112.96(8)
N(2)−Zn(1)−O(2)[a]	97.13(6)	O(2)−P(2)−C(39)	109.37(9)
N(3)−Zn(1)−N(4)	87.66(6)	O(2)−P(2)−C(45)	111.44(8)
N(3)−Zn(1)−O(2)[a]	97.91(6)	C(15)−P(2)−C(39)	114.41(8)
N(4)−Zn(1)−O(2)[a]	102.76(6)	C(15)−P(2)−C(45)	105.83(9)
O(1)−P(1)−C(5)	113.80(9)	C(39)−P(2)−C(45)	102.30(9)
		P(2)[1]−O(2)[1]−Zn(1)	177.56(9)

[a] $-x + 1, y - 1/2, -z + 1/2$.

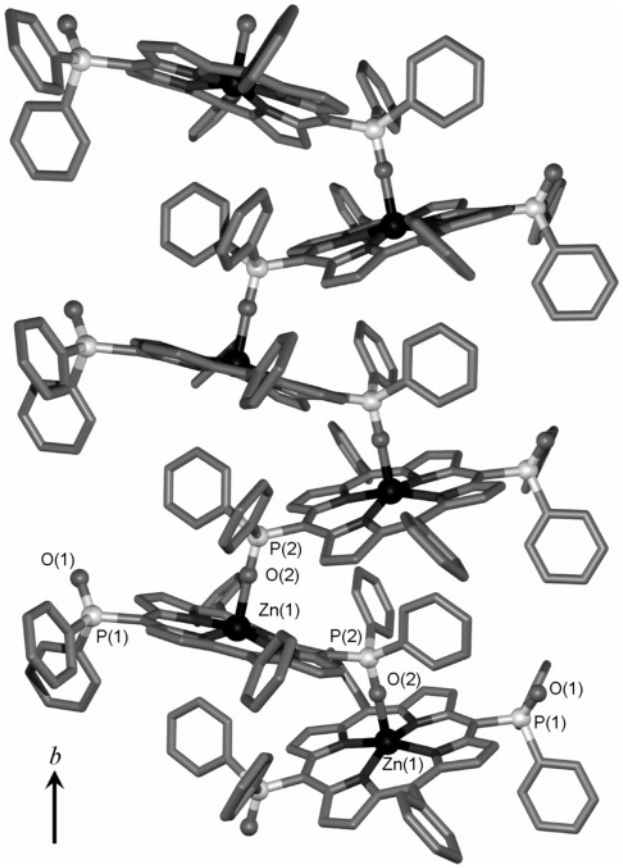

Figure 8. Section of the one-dimensional coordination polymer in {[10,20-diphenylporphyrinatozinc(II)-5,15-diyl]-bis-[P(O)Ph$_2$]}$_n$·{1.5H$_2$O}$_n$.

complex. This coordination configuration propagates along the crystallographic *b* axis to produce a chainlike, one-dimensional, coordination polymer, as illustrated in Figure 8. The oxygen atom [O(1)] of the second diphenylphosphine oxide group plays no part in proliferation of the polymer but rather is directed into a cavity in the lattice that is also occupied by disordered water molecules [PO···O_{water} distances range between 2.61 and 3.47 Å for O(1w), O(2w), O(3w), and O(4w)]. Contact distances to the other partial

(54) Senge, M. O. *Chem. Commun.* **2006**, 243−256.
(55) Farrugia, L. J. *J. Appl. Crystallogr.* **1997**, *30*, 565.

occupancy water sites are too long to be considered significant H-bond interactions. The cavity containing the disordered water molecules is surrounded on all other sides by hydrophobic phenyl rings of the ligands.

The phenyl rings (and therefore the oxygen atoms) of the two diphenylphosphine oxide groups protrude on opposite sides of the mean plane of the macrocycle in a trans-like arrangement. The carbon framework of the porphyrin ring is distorted from planarity. The maximum deviation from the mean plane of the ring occurs for the β-carbon C(17) at 0.42 Å. Of interest with respect to molecular geometry is the almost linear bonding configuration around the coordinated diphenylphosphine oxide oxygen atom O(2) [P(2)−O(2)−Zn(1) = 177.56(9)°]. Similar compounds in the literature show bond angles between 140° and 180° for analogous phosphine oxide coordinating groups, so this situation is not considered abnormal.[56]

The phenyl rings of the diphenylphosphine oxide groups bound to zinc are sandwiched by alternating pairs of porphyrin rings in the chain. There are intrachain aryl−aryl interactions of the edge-to-face type between the edges of the diphenylphosphine oxide phenyl rings [C(39)−C(44) and C(45)−C(50)] and the faces of the aromatic porphyrin rings ($CH_{edge}\cdots Porphyrin_{plane}$ contact distances between 2.65 and 2.80 Å). Each phenyl ring is involved in two edge-to-face interactions, and as such, these contacts bridge alternating porphyrin rings within the chain. The contact distances are quite short and may be responsible for some of the distortion observed for the carbon framework of the macrocycles.

There are notable interchain aryl−aryl interactions that involve both diphenylphosphine oxide phenyl rings and the meso substituent phenyl rings of the macrocycle. Adjacent chains are connected to one another by vertex-to-face-type interactions between the meso phenyl rings comprising C(33)−C(38) (vertex) and the diphenylphosphine oxide phenyl rings comprising C(21)−C(26) (face) ($CH_{vertex}\cdots Ph_{plane}$ = 3.10 Å) that propagate the lattice in the *c* direction. Also, connecting adjacent chains in the *c* direction are offset face-to-face π-stacking interactions between meso phenyl rings [C(51)−C(56)]. Each ring is involved in two such interactions, with interaction distances $Ph_{plane}\cdots Ph_{plane}$ = 3.53 and 3.61 Å, which form a continuous thread, normal to the *ac* plane, that propagates with crystallographic inversion symmetry.

Other aryl−aryl interactions connect adjacent coordinate polymer chains in the third dimension (parallel to the *a* axis). The diphenylphosphine phenyl ring comprising C(27)−C(32) is involved in two interactions; one being an offset face-to-face interaction with the diphenylphosphine phenyl ring C(45)−C(50) (mean $Ph_{plane}\cdots Ph_{plane}$ = 3.4 Å) and the other, a vertex-to-face interaction with C(39)−C(44). There are other, longer-range interactions, but these do not warrant particular mention.

Conclusions

Several representatives of a new class of porphyrins with one and two diphenylphosphine oxide substituents in the meso position(s) have been prepared in very good to excellent yields by both stoichiometric and palladium-catalyzed reactions. Their structures have been demonstrated unambiguously by various spectroscopic techniques and single-crystal structures. As part of their investigation into the potential applications of porphyrins as molecular tectons, Deiters et al.[57] report a similar coordination polymer motif for zinc complexes of porphyrins bearing coordinating pyridine *N*-oxide groups (as opposed to the coordinating diphenylphosphine oxide groups in the present study). This motif may be a recurring one and therefore be applicable to crystal engineering by functional group variation. In the future, we will be investigating the complexation properties of our new phosphine oxides in solution. There is also scope for the construction of more elaborate coordination frameworks based on these bis-diphenylphosphine oxide porphyrin ligands by combination with metals that adopt six-coordinate configurations [e.g., Cr(III), Ru(II), Os(II)] when complexed with porphyrinoid ligands. In addition, we propose that these phosphine oxides could be utilized as interesting new ligands for non-porphyrinic organometallic and inorganic centers.

Acknowledgment. F.A. would like to thank the Department of Education, Science and Training (DEST) and the Faculty of Science, Queensland University of Technology for Post-Graduate Scholarships.

Supporting Information Available: CIF files for compounds **14** and **16**. This material is available free of charge via the Internet at http://pubs.acs.org.

IC060372U

(56) Inamo, M.; Matsubara, N.; Nakajima, K.; Iwayama, T. S.; Okimi, H.; Hoshino, M. *Inorg. Chem.* **2005**, *44*, 6445−6455.

(57) Deiters, E.; Bulach, V.; Kyritsakas, N.; Hosseini, M. W. *New J. Chem.* **2005**, *29*, 1508−1513.